

Tetranuclear copper(II) complexes incorporating short and long metal–metal separations: synthesis, structure and magnetism†

Paul E. Kruger,^{a*} Boujemaa Moubaraki,^b Gary D. Fallon^b and Keith S. Murray^b

^a Department of Chemistry, Trinity College, Dublin 2, Ireland. E-mail: Paul.Kruger@tcd.ie

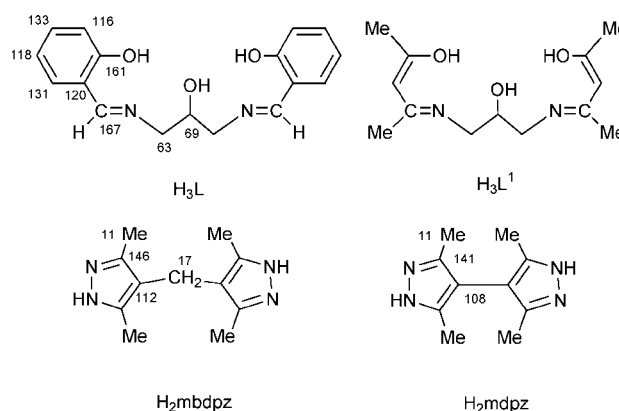
^b Department of Chemistry, Monash University, Clayton, Victoria 3168, Australia

Received 12th October 1999, Accepted 12th January 2000

Synthesis, structural and magnetic characterization of tetranuclear $[(\text{Cu}_2\text{L})_2\text{B}]$ complexes [where H_3L is the Schiff's-base ligand, 1,3-bis(salicylideneamino)propan-2-ol; B is the dipyrazolate entities: methylenebis(3,5-dimethylpyrazolate) (mbdpz) or 4,4'-bi-3,5-dimethylpyrazolate (mdpz)] are reported. The structures reveal short intra- and inter-molecular $\text{Cu} \cdots \text{Cu}$ separations (*ca.* 3.4 Å), in combination with long intramolecular copper distances (*ca.* 10 Å). The magnetic behaviour of $[(\text{Cu}_2\text{L})_2(\text{mbdpz})]$ (**1**) is indicative of an intramolecular antiferromagnetic interaction between the copper(II) centres [$2J = -460 \text{ cm}^{-1}$], whilst that of $[(\text{Cu}_2\text{L})_2(\text{mdpz})]$ (**2**) is characteristic of an antiferromagnetically coupled system with intramolecular coupling in the order of $2J = -380 \text{ cm}^{-1}$, with the presence of a further intermolecular interaction indicated.

Protein crystallographic and detailed spectroscopic studies of a number of enzymes containing polymetallic active sites have shown the occurrence of small clusters of metal ions, with short metal–metal separations (*e.g.* <3.6 Å), together with other clusters or single-metal ion sites, situated a much larger distance away in the protein matrix (*e.g.* >10 Å).¹ Such structural motifs have been identified within the multi-copper oxidases.² Laccase and ascorbate oxidase possess oxygen binding trinuclear clusters, T2 plus T3, a large distance away (*ca.* 13 Å) from the substrate oxidation/electron transfer T1 copper site. The hexa-copper ceruloplasmins possess a similar topology but contain two additional T1 sites *ca.* 18 Å from T1. In addition, the 8-Fe ferredoxins contain two cubane clusters spaced *ca.* 12 Å apart and, more recently identified, the Fe–Mo cofactor of the nitrogenase enzyme contains a metal cluster possessing both short and long metal–metal separations.³ We have been developing a strategy aimed at incorporating metal centres into multi-metallic complexes such that they are both in close proximity to each other and at much further distances away (within 3–4 Å and at ≥10 Å). This is in an attempt to mimic the topology found in the above native systems.

Several methods may be employed in the synthesis of poly-metallic coordination compounds and include, amongst others, the self-assembly or aggregation of metal centres and ligand species, both coordinating and bridging, into poly-metallic arrays;⁴ or the direct incorporation of metal ions into preformed polydentate ligands.⁵ This second approach offers many potential advantages over the self-assembly route in that it enables more stringent control over the course of the reaction and upon the products that form. We have favoured a 'pair-of-dimers' approach to form tetranuclear complexes through the employment of preformed dinucleating ligands (L). In this method $[\text{M}_2\text{L}]$ units are connected through bridging ligands to form $[\text{M}_2\text{L}]_2$ compounds. We have utilized a range of dinucleating Schiff's-base ligands built on a propan-2-ol backbone and successfully incorporated first row transition metals within their coordination cavities.⁶ Linking $[\text{M}_2\text{L}]$ units with dipyrazolate bridging ligands gives 'pairs-of-dimers' $[\text{M}_2\text{L}]_2$.⁷ We extend this series in the present study and report full preparative, structural and magnetic details of tetranuclear, $[(\text{Cu}_2\text{L})_2(\text{mbdpz})]$ (**1**) and $[(\text{Cu}_2\text{L})_2(\text{mdpz})]$ (**2**).



Experimental

Materials and methods

Solvents and chemicals were of laboratory grade and were used as received. Acquisition of infrared, ultraviolet-visible, mass, δ_{H} and δ_{C} NMR spectra were performed as detailed previously.⁶ Abbreviations have their usual meaning. Chemical analyses; C, H, N were performed by the Commonwealth Micro-Analytical Services, Melbourne, Australia. Magnetic measurements at room temperature were performed using a Faraday balance which incorporated a Newport electromagnet fitted with Faraday-profile pole faces. Diamagnetic corrections for ligand susceptibilities were made using Pascal's constants. Variable-temperature magnetic susceptibility measurements (300–4.2 K) were performed on powdered samples at a field strength of 10 000 G (1 T) using a Quantum Design M.P.M.S. Squid magnetometer.⁸

Crystallographic measurements on **1** and **2**

Crystal data and experimental details are summarized in Table 1. The structures of **1** and **2** were solved by direct methods.⁹ CCDC reference number 186/1801.

See <http://www.rsc.org/suppdata/ft/a9/a908177a/> for crystallographic files in .cif format.

Synthesis of 1,3-bis(salicylideneamino)propan-2-ol, H_3L

The method of Mazurek¹⁰ was employed in the synthesis of

† Dedicated to the memory of Professor Olivier Kahn, a leading light in the field of molecular magnetism.

Table 1 Crystallographic details for [(Cu₂L)₂(mbdpz)] (**1**) and [(Cu₂L)₂(mdpz)] (**2**)

	1	2
Chemical formula	Cu ₄ C ₄₅ H ₄₄ N ₈ O ₆	Cu ₄ C ₄₄ H ₄₂ N ₈ O ₆
Formula weight	1047.1	1033.1
Crystal system	Monoclinic	Triclinic
Space group	C2/c	P $\bar{1}$
μ (Cu-K α)/cm ⁻¹	28.8	27.9
<i>a</i> /Å	14.495(3)	18.630(2)
<i>b</i> /Å	17.395(2)	12.459(1)
<i>c</i> /Å	16.334(2)	9.319(1)
α /°	—	81.546(8)
β /°	100.98(1)	86.965(6)
γ /°	—	76.897(8)
<i>V</i> /Å ³	4043(1)	2083.4(4)
<i>Z</i>	4	2
<i>T</i> /K	293.2	293.2
<i>R</i> _{int}	0.024	0.019
<i>R</i> , <i>wR</i> 2 (obs. data)	0.039, 0.048	0.039, 0.049
<i>R</i> , <i>wR</i> 2 (all data)	0.057, 0.065	0.055, 0.064
Reflections:		
measured	6515	6546
independent	3011	6185
observed	2287	4682

H₃L, the product being recrystallized from methanol. Full characterisation is reported here. Mp 101–103 °C. Found: C, 68.3; H, 6.3; N, 9.2%. C₁₇H₁₈N₂O₃: requires C, 68.4; H, 6.1; N, 9.4%. λ_{\max} /nm (MeOH) 215 (ϵ /dm³ mol⁻¹ cm⁻¹ 41500), 250 (22000), 315 (7200) and 400 (2350). ν_{\max} /cm⁻¹ (Nujol) 3394s (br), 1635s, 1611m, 1579m, 1497m, 1339w, 1275s, 1207w, 1156w, 1104w, 1084w, 1048m, 1036w, 1025m, 973w, 940w, 844m (br), 771m, 752s, 738m, 661w. *m/z* 298 (M⁺, 30%), 164 (100), 135 (70). δ_{H} (CDCl₃, 300 MHz): 8.25 (2H, s, imine), 7.30 (4H, m, phenyl), 6.80 (4H, m, phenyl), 4.15 (1H, m, CH–O) and 3.60 (4H, m, CH₂). δ_{C} (CDCl₃, 75 MHz): 167 (C7), 161 (C1), 133 (C3), 131 (C5), 120 (C6), 118 (C4), 116 (C2), 69 (C9) and 63 (C8).

Synthesis of methylenebis(3,5-dimethylpyrazole) (H₂mbdpz)

Methylenebis(3,5-dimethylpyrazole) was prepared from 3,5-diacetylheptane-2,6-dione which in turn was prepared *via* a modification of the method of Knövenagel¹¹ from acetylacetone and formaldehyde.

3,5-Diacetylheptane-2,6-dione. To an ice cold solution of acetylacetone (20 g, 0.20 mol) and formaldehyde (7.2 g, 0.24 mol), was added with vigorous stirring, four drops of diethylamine. The mixture was stirred for 24 h at room temperature and an additional four drops of diethylamine added. This procedure was repeated for the following five days. After this time an aqueous and organic phase were evident. The organic phase was separated and extracted with diethyl ether and dried over MgSO₄. The ethereal solution was cooled in an acetone/dry ice bath to precipitate a white solid which was filtered off at low temperature. A pale yellow oil results on standing the filtrate at room temperature. Yield 90%. Found: C, 62.4; H, 7.8%. C₁₁H₁₆O₄: requires C, 62.2; H, 7.6%. ν_{\max} /cm⁻¹ (Nujol): 1720–1680vs (br), 1430s, 1355m, 1330sh, 1315m, 1290m, 1155vs, 1030sh, 960m (br) and 740w. δ_{H} (CDCl₃, 200 MHz): 2.1–2.4 (14H, m, CH₃ and CH₂) and 3.8 (2H, t, CH).

4,4'-Methylenebis(3,5-dimethylpyrazole) (H₂mbdpz). 3,5-Diacetylheptane-2,4-dione (12.0 g, 0.055 mol) dissolved in 20 ml of ethanol was added cautiously to 13 ml of hydrazine hydrate (98% soln.) with stirring at ambient temperature. The reaction mixture was then refluxed for 45 min and stirred at room temperature for an additional 18 h. The resultant white solid was filtered off, washed with water and dried *in vacuo*. Yield 10 g, 90%. Mp 275–277 °C. Found: C, 64.5; H, 8.1; N, 27.2%. C₁₁H₁₆N₄: requires C, 64.7; H, 7.9; N, 27.4%. ν_{\max} /cm⁻¹

(Nujol): 3185vs, 3130vs, 3081vs, 1620w (sh), 1589s, 1516w, 1418s, 1300s, 1207w, 1152m, 1079w, 1030m, 1000w (sh), 876w (sh), 840s, 798m and 750m. *m/z* 204 (M⁺, 50%), 189 (30), 108 (100) and 97 (30). δ_{H} (DMSO-*d*₆, 200 MHz): 2.0 (12H, s, CH₃), 3.35 (2H, s, CH₂) and 11.9 (2H, s, br, NH). δ_{C} (DMSO-*d*₆, 50 MHz): 146 (C2), 112 (C3), 17 (C4) and 11 (C1).

Synthesis of 4,4'-bi-3,5-dimethylpyrazole (H₂mdpz)

4,4'-Bi-3,5-dimethylpyrazole was prepared from the tetra-ketone intermediate, 3,4-diacetylhexane-2,5-dione, by a slight modification to the method of Mosby.¹²

3,4-Diacetylhexane-2,5-dione. Acetylacetone (100 g, 1.0 mol) was added dropwise, over a period of 6 h under a nitrogen atmosphere, to a diethyl ether slurry of NaH (24 g, 1.0 mol). A further amount of ether was added and the mixture heated so as to extract iodine (127 g, 1.0 mol) from a Soxhlet thimble placed below the condenser. On completion of the iodine extraction the mixture was allowed to cool, and was filtered and the solid washed with ether so as to remove any excess iodine present. The resultant white solid was recrystallized from acetic acid to retrieve a white crystalline product in 65% yield. Mp 190–191 °C. Found: C, 60.4; H, 7.0%. C₁₀H₁₄O₄: requires C, 60.6; H, 7.1%. ν_{\max} /cm⁻¹ (KBr) 1630–1520 s (br), 1410m, 1370w (sh), 1260s, 1025vs and 1000s. *m/z* 198 (M⁺ 50%), 180 (70), 165 (100), 123 (50) and 113 (20). δ_{H} (CDCl₃, 200 MHz): 2.0 (12H, s, CH₃). δ_{C} (CDCl₃, 50 MHz): 192 (C2), 108 (C3) and 23.5 (C1).

4,4'-Bi-3,5-dimethylpyrazole (H₂mdpz). 3,4-Diacetylhexane-2,5-dione (9.9 g, 0.05 mol) was added portionwise to hydrazine hydrate (15 ml of an 85% aqueous solution) as expeditiously as possible (**CAUTION!** highly exothermic reaction). The mixture was cooled in ice, the precipitate filtered off and washed with ice cold water. The solid was dissolved in hot methanol and water added to induce reprecipitation of a microcrystalline white powder which was collected and dried under high vacuum. Yield 5.5 g, 58%. Mp 300 °C. Found: C, 62.9; H, 7.2; N, 29.2%. C₁₀H₁₄N₄: requires C, 63.1; H, 7.4; N, 29.4%. ν_{\max} /cm⁻¹ (Nujol) 3172s (br), 3050s, 1685w (br), 1618m, 1576m, 1532m, 1420s, 1302s, 1258m, 1157m, 1138m, 1063w, 1017vs, 972 (sh), 830 (sh) (br), 783vs, 700sh (br) and 625w. *m/z* 190 (M⁺, 100%), 175 (20) and 148 (35). δ_{H} (DMSO-*d*₆, 200 MHz): 2.0 (12H, s, CH₃) and 12.7 (2H, s, br, NH). δ_{C} (DMSO-*d*₆, Cr(acac)₃, 50 MHz): 141 (C2, br), 108 (C3) and 11 (C1).

Synthesis of (1) and (2)

The compounds were prepared by using a modification to the procedure reported previously by Mazurek.¹³ The dipyrazole entities were used in place of pyrazole, with relevant adjustment being made for reactant stoichiometry. The following preparation of **1** is representative.

A methanolic solution of H₃L (2.98 g, 0.01 mol) was slowly added to a stirred methanolic solution containing H₂mbdpz (1.02 g, 0.005 mol) and copper(II) nitrate trihydrate (4.832 g, 0.02 mol). After dissolution was complete, a methanolic solution of potassium hydroxide (2.24 g, 0.04 mol) was added with vigorous stirring. Stirring continued for a further 20 min, resulting in the full development of a deep blue-green coloured precipitate. The mixture was filtered to remove the precipitate, which was subsequently washed with water (2 × 50 ml), methanol (2 × 20 ml), acetone (2 × 20 ml) and air dried. The solid was purified by Soxhlet extraction (CHCl₃/CH₂Cl₂) over a period of 3 days. The resultant solution was reduced in volume to complete the precipitation of the blue-green coloured microcrystalline solid, which was collected, washed with diethyl ether and air dried. Recrystallization of the products from dimethylformamide yielded dark aquamarine coloured crystalline compounds. The crystals used for the structural determinations of **1** and **2** were grown by vapour diffusion of diethyl ether into a

dimethylformamide/dimethyl sulfoxide solution of the respective compounds.

[(Cu₂L)₂(mbdpz)] (1). Yield 73%. Found: C, 51.6; H, 4.2; N, 10.7%. Cu₄C₄₅H₄₄N₈O₆: requires C, 51.4; H, 4.3; N, 10.8%. λ_{max} /nm (CHCl₃) 378 (ϵ /dm³ mol⁻¹ 26050) and 600 (1189). ν_{max} /cm⁻¹ (Nujol) 1630vs, 1598s, 1532m, 1448vs, 1392m, 1345m, 1308s, 1210w (sh), 1195m, 1144m, 1125m, 1080w, 1058m, 1030w, 990w, 967w, 911w (sh), 893m, 858w, 793m, 755vs, 720m and 670m. μ_{eff} (295 K) = 1.16 μ_{B} per Cu.

[(Cu₂L)₂(mdpz)] (2). Yield 68%. Found: C, 51.1; H, 4.0; N, 10.8%. Cu₄C₄₄H₄₂N₈O₆: requires C, 50.9; H, 3.8; N, 11.0%. λ_{max} /nm (CHCl₃) 376 (ϵ /dm³ mol⁻¹ 26428) and 601 (1211). ν_{max} /cm⁻¹ (Nujol) 1630vs, 1599s, 1537s, 1448vs, 1385m, 1330m, 1315s, 1309s, 1280w, 1240w, 1210w (sh), 1194m, 1149m, 1126m, 1088w, 1050m (sh), 1039s, 961w, 908w, 894m, 790w, 750s, 719s and 668m. μ_{eff} (295 K) = 1.22 μ_{B} per Cu.

Results and discussion

Synthesis and characterization

The synthesis of the tetranuclear copper complexes followed a general procedure in which methanolic solutions of the divalent metal salts, H₃L and the respective dipyrazole entity, were treated with a methanolic solution of potassium hydroxide, resulting in the immediate precipitation of the product. Recrystallization was achieved through Soxhlet extraction, over a period of days, of the solids obtained into a CH₂Cl₂/CHCl₃ solvent mix. The tetranuclear Cu(II) complexes are blue-green in appearance giving similarly coloured solutions when dissolved in DMF or chloroform and this is in accord with planar geometry around the metal atoms.¹⁴

Crystal structure of 1

The dinucleating pentadentate character of the ligand and the desired pair-of-dimers arrangement, through the incorporation of the dipyrazolate moiety within the exogenous bridge, is clearly evident and is shown in Fig. 1. The molecule possesses a two-fold axis of symmetry through C(23) and each dinucleating half is rotated by 10° relative to the other at this atom. This is probably due to non-bonded interactions between the methyl groups and the protons of the methylene bridge.¹⁵ The copper atoms are coordinated in slightly distorted square planar arrangements within each dinucleating half of the complex and bridged mono-atomically by the secondary alkoxo oxygen of the ligand and di-atomically by the pyrazolato moiety. The dihedral angle between the [CuN₂O₂] chromophores is 169.0° and consequent bending of the molecule from coplanarity is evident. The intramolecular distance between Cu(1) and Cu(2) is 3.391(1) Å, which is slightly longer than those within **2** (3.373(1) Å see below), but falls within the range of distances found for this and related pyrazolato-bridged dinuclear copper species.^{13,16} The Cu(1)–O(1)–Cu(2) bridging angle is 126.5(2)° and the angle at which the plane of the pyrazolate ring of the mbdpz molecule intersects the plane encompassing the Cu(1)–O(1)–Cu(2) bridge is 163.1°. The pertinent across-mbdpz intramolecular copper-to-copper separations are, Cu(1)···Cu(1A) 10.446(1) Å, Cu(2)···Cu(2A) 9.459(2) Å and Cu(1)···Cu(2A) 9.456(1) Å. Intermolecular copper-to-copper separations are significantly shorter than the across dipyrazole (mbdpz) Cu···Cu separations. This is brought about by the phenoxy oxygens, O(2A) and O(2B), bridging between Cu(1A) and Cu(1B) and forming a tetranuclear copper centre Fig. 1(b). Further important bond lengths and angles are given in Table 2.

Crystal structure of 2

The desired pair-of-dimers arrangement is clearly evident and

Table 2 Selected bond lengths (Å) and angles (°) for [(Cu₂L)₂(mbdpz)] (1)

Cu(1)–O(1)	1.895(3)	Cu(1)–O(2)	1.923(3)
Cu(1)–N(2)	1.972(4)	Cu(1)–N(3)	2.020(4)
Cu(2)–O(1)	1.901(3)	Cu(2)–O(3)	1.910(3)
Cu(2)–N(1)	1.964(4)	Cu(2)–N(4)	1.989(4)
Cu(1)···Cu(2)	3.391(1)	Cu(1)···Cu(2A)	9.456(1)
Cu(1)···Cu(1A)	10.446(1)	Cu(2)···Cu(2A)	9.459(2)
Cu(1)···Cu(1B)	3.431(1)	Cu(2)···Cu(2B)	4.063(1)
Cu(1A)···O(2B)	2.590(2)		
O(1)–Cu(1)–O(2)	172.2(1)	O(1)–Cu(2)–O(3)	170.7(1)
O(1)–Cu(1)–N(2)	82.3(1)	O(1)–Cu(2)–N(1)	82.6(2)
O(1)–Cu(1)–N(3)	85.9(1)	O(1)–Cu(2)–N(4)	86.5(1)
O(2)–Cu(1)–N(2)	91.3(1)	O(3)–Cu(2)–N(1)	90.6(2)
O(2)–Cu(1)–N(3)	101.3(1)	O(3)–Cu(2)–N(4)	101.5(1)
N(2)–Cu(1)–N(3)	162.9(2)	N(1)–Cu(2)–N(4)	162.9(2)
Cu(1)–O(1)–Cu(2)	126.5(2)		

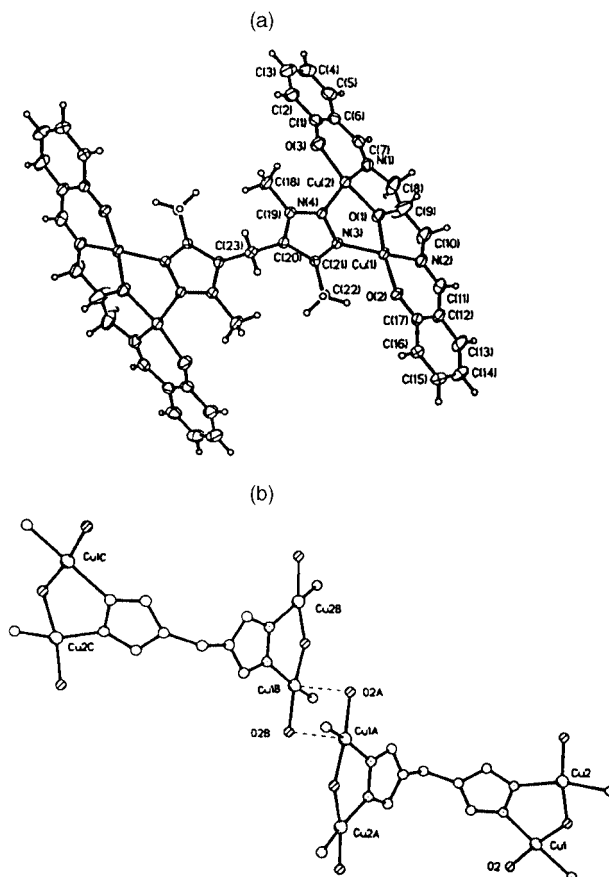


Fig. 1 (a) Molecular structure and atomic numbering scheme for **1**. Thermal ellipsoids are shown at the 40% level. (b) The coordination chromophores and bridging ligand (mbdpz, methyl groups omitted for clarity) of **1** showing the intermolecular association of Cu(1A) and Cu(1B) through the phenoxy oxygens O(2A) and O(2B).

shown in Fig. 2. Important bond lengths and angles are given in Table 3. The Cu···Cu separations within each half are Cu(1)···Cu(2) 3.373(1) Å and Cu(3)···Cu(4) 3.368(1) Å, and are slightly shorter than those found in **1** (see above). The complex possesses a distinct twisting around the central C(20)–C(42) bond, ($\approx 68^\circ$), generated by an interaction of the 3,3' and 5,5' methyl groups on the mdpz rings, and compares with the rotation of $\approx 58^\circ$ found in [(Ni₂L¹)₂(mdpz)].⁷ The overall molecular geometry consists of two non-identical halves bridged by the mdpz moiety. The disparity is made evident through noting the following: (i) the bridging angle, Cu–O–Cu, within each half of the complex is slightly different, Cu(1)O(1)Cu(2) 127.0(1)°, Cu(3)O(4)Cu(4) 126.0(1)°; (ii) the dihedral angle between each [CuN₂O₂] chromophore is different, [Cu(1)N₂O₂–Cu(2)N₂O₂] 176.6° and [Cu(3)N₂O₂–Cu(4)–

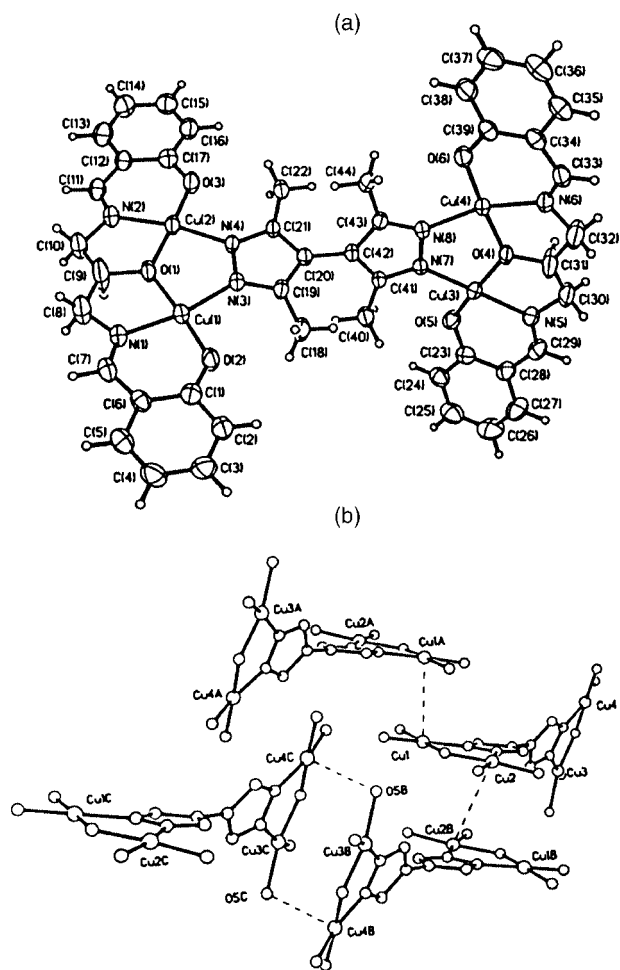


Fig. 2 (a) Molecular structure and atomic numbering scheme for **2**. Thermal ellipsoids are shown at the 40% level. (b) The coordination chromophores and bridging ligand (mdp, methyl groups omitted for clarity) of **2** showing the intermolecular stacking association of Cu(1) and Cu(2) with Cu(1A) and Cu(2B), respectively and of Cu(3B) and Cu(4B) with Cu(4C) and Cu(3C), respectively.

N_2O_2 169.9°; (iii) the angle at which the plane of each mdp pyrazolate ring intersects the plane encompassing the Cu–O–Cu bridge differs by some 15°, $[\text{N}(3)\text{N}(4)\text{C}(19)\text{C}(20)\text{C}(21)]$ – $[\text{Cu}(1)\text{O}(1)\text{Cu}(2)]$ 175.1° and $[\text{N}(7)\text{N}(8)\text{C}(41)\text{C}(42)\text{C}(43)]$ – $[\text{Cu}(3)\text{O}(4)\text{Cu}(4)]$ 160.3°, thus the mdpz bridging between Cu(1) and Cu(2) is essentially coplanar with the dinuclear fragment containing them, whereas the bridging between Cu(3) and Cu(4) is quite removed from coplanarity and; (iv) the intermolecular interactions experienced by Cu(1) and Cu(2) are different to those of Cu(3) and Cu(4) as shown in Fig. 2(b). This results in the intermolecular Cu...Cu separations being smaller (*ca.* 3.4–4.3 Å) than across mdpz separations, which are in the order of 10 Å. Further distortions about the metal centres are also evident and are indicated within Table 3.

Magnetic exchange in **1** and **2**

Variable temperature magnetic susceptibility studies were carried out on powdered samples of the complexes over the temperature range 4.2–300 K. As is commonly observed within complexes possessing an antiferromagnetic interaction between metal centres, the presence of a monomeric impurity is evident at low temperatures, through a slight increase in χ_{Cu} . The data were first treated by applying a modified Bleaney–Bowers¹⁷ equation, calculated for two $S = 1/2$ centres under a $-2J\hat{S}_1 \times \hat{S}_2$ spin Hamiltonian, using a non-linear least-squares fitting routine. The susceptibility equation (1) allowed for the presence

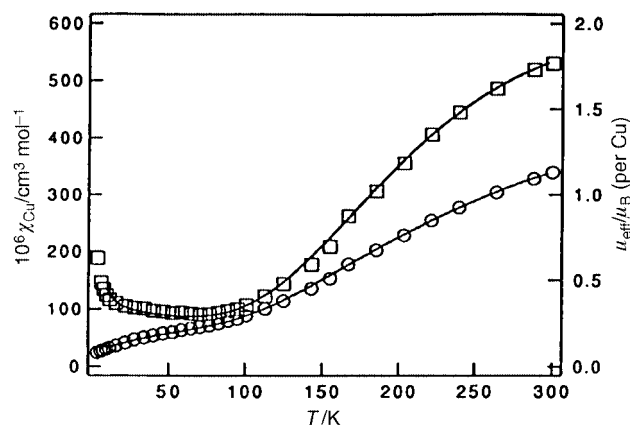


Fig. 3 Temperature dependence of the magnetic susceptibility (\square) and magnetic moment (\circ) for **1**. The solid line is that calculated using eqn. (1) using the parameters outlined in the text.

$$\chi_{\text{Cu}} = \frac{Ng^2\beta^2}{kT} \left[3 + \exp\left(\frac{-2J}{kT}\right) \right]^{-1} (1 - P) + \frac{Ng^2\beta^2 P}{4kT} + N_a \quad (1)$$

of a percentage of monomeric impurity that was assumed to have the same g -value as the complex.

All the symbols have their usual meaning and P is the fraction of monomeric impurity.

[(Cu₂L)₂(mbdpz)] (1**).** The μ_{Cu} values decrease from 1.16 μ_{B} at 300 K to 0.1 μ_{B} at 4.2 K and are shown graphically in Fig. 3. It is evident from Fig. 3 that the compound is experiencing a moderately strong antiferromagnetic interaction between the metal centres within the $[\text{Cu}_2\text{L}]$ fragments. The data were fitted first to eqn. (1) and this assumed that the two dinuclear moieties had no cross-mbdpz coupling as would be expected. An excellent fit was obtained (Fig. 3) using the parameter values $g = 2.10$, $2J = -460 \text{ cm}^{-1}$, $P = 0.016$, $N_a = 60 \times 10^{-6} \text{ cm}^3 \text{ mol}^{-1}$ per Cu. This $2J$ value is larger than that of the related μ -pyrazolato bridged dinuclear complex $[\text{Cu}_2\text{L}(\text{pz})]$ ($2J = -240 \text{ cm}^{-1}$) which has $r(\text{Cu}–\text{Cu}) = 3.359(4) \text{ \AA}$ and a $\text{Cu}(1)–\text{O}–\text{Cu}(2)$ angle of $125.1(7)^\circ$, both slightly smaller than in **1**.¹⁸ In order to see if any intermolecular coupling occurs in **1**, between Cu(1A) and Cu(1B) through the phenoxy oxygens O(2A) and O(2B), the data were fitted to a tetramer model developed by Hatfield and Inman,¹⁹ to treat dinuclear copper(II) Schiff-base complexes paired weakly together *via* 90° phenoxo bridges. The intermolecular J value of interest in their model (J_{12} short diagonal), is equivalent to $J_{1A,1B}$ in **1**. The other intermolecular couplings (J_{14} and J_{34} in ref. 19) were set to zero since there are no direct bridging pathways. It was found upon varying this $J_{1A,1B}$ parameter from $+50 \text{ cm}^{-1}$ to -50 cm^{-1} , while keeping the intra-dinuclear parameter J and g values constant at the above values, or when allowing J and g also to vary, that $J_{1A,1B}$ had only a very small effect on the quality of the fit. Thus $J_{1A,1B}$ equal to $+50 \text{ cm}^{-1}$ gave calculated χ values a little larger than observed above 200 K, while use of $J_{1A,1B}$ of -50 cm^{-1} gave calculated values slightly less than observed above 200 K. Thus $J_{1A,1B} = 0$ remains the best-fit. Other related ‘pair-of-dimer’ species, having weak phenoxo bridges also show either positive or negative values close to zero.²⁰

[(Cu₂L)₂(mdpz)] (2**).** The μ_{B} values decrease from 1.22 μ_{B} at 300 K to 0.1 μ_{B} at 4.2 K. Though a maximum is not evident below 300 K, within the corresponding susceptibility plot, the general appearance is that of a compound possessing a medium to strong antiferro-magnetic interaction between the paramagnetic centres. In attempting to fit the data, employment of an isolated dimer model (single J value) of the type described above gave a reasonable fit using $2J$ of *ca.* -380 cm^{-1} , with

Table 3 Selected bond lengths Å and angles (°) for [(Cu₂L)₂(mdpz)] (**2**)

Cu(1)–O(1)	1.884(3)	Cu(2)–O(1)	1.889(3)
Cu(3)–O(4)	1.883(3)	Cu(4)–O(4)	1.897(3)
Cu(1)–O(2)	1.880(3)	Cu(2)–O(3)	1.886(3)
Cu(3)–O(5)	1.901(3)	Cu(4)–O(6)	1.886(3)
Cu(1)–N(1)	1.961(4)	Cu(2)–N(2)	1.945(4)
Cu(3)–N(5)	1.957(4)	Cu(4)–N(6)	1.955(3)
Cu(1)–N(3)	2.005(4)	Cu(2)–N(4)	1.998(3)
Cu(3)–N(7)	1.985(3)	Cu(4)–N(8)	2.006(3)
Cu(1)···Cu(2)	3.373(1)	Cu(3)···Cu(4)	3.368(1)
Cu(1)···Cu(1A)	3.772(1)	Cu(2)···Cu(2B)	3.693(1)
Cu(3B)···Cu(3C)	3.477(1)	Cu(4B)···Cu(4C)	4.284(1)
Cu(3B)···Cu(4C)	3.701(1)	Cu(4B)···O(5C)	2.731(1)
O(2)–Cu(1)–O(1)	175.1(1)	O(3)–Cu(2)–O(1)	174.3(1)
O(4)–Cu(3)–O(5)	166.8(1)	O(4)–Cu(4)–O(6)	174.8(1)
O(2)–Cu(1)–N(1)	92.7(2)	O(3)–Cu(2)–N(2)	92.8(2)
O(4)–Cu(3)–N(5)	82.6(1)	O(4)–Cu(4)–N(6)	82.5(1)
O(2)–Cu(1)–N(3)	97.6(1)	O(3)–Cu(2)–N(4)	97.7(1)
O(4)–Cu(3)–N(7)	87.0(1)	O(4)–Cu(4)–N(8)	86.5(1)
O(1)–Cu(1)–N(1)	82.8(1)	O(3)–Cu(2)–N(2)	92.8(1)
O(5)–Cu(3)–N(5)	91.8(1)	O(6)–Cu(4)–N(6)	92.3(1)
O(1)–Cu(1)–N(3)	86.9(1)	O(1)–Cu(2)–N(4)	86.9(1)
O(5)–Cu(3)–N(7)	100.7(1)	O(6)–Cu(4)–N(8)	98.7(1)
N(1)–Cu(1)–N(3)	169.3(2)	N(2)–Cu(2)–N(4)	169.4(2)
N(5)–Cu(3)–N(7)	164.5(1)	N(6)–Cu(4)–N(8)	163.5(2)
Cu(1)–O(1)–Cu(2)	127.0(1)	Cu(3)–O(4)–Cu(4)	126.0(1)
Cu(2)–Cu(1)–Cu(1A)	87.20(3)	Cu(1)–Cu(2)–Cu(2B)	80.93(3)
Cu(4B)–Cu(3B)–Cu(3C)	65.45(2)	Cu(4B)–Cu(3B)–Cu(4C)	121.30(2)
Cu(3C)–Cu(3B)–Cu(4C)	55.86(2)	Cu(3B)–Cu(4B)–Cu(3C)	58.70(2)

$g = 2.05$ and $P = 0.01$, but there were divergences between the observed and calculated χ values. Various attempts were made to improve the fit while taking into account both the small structural differences between each dinuclear half of **2** and the intermolecular interactions. While the latter interactions are complex (see above), a first approximation to probing their effect was to use the Hatfield and Inman tetramer model,¹⁹ described above. This is appropriate to the parallelogram interaction between Cu(3B)···Cu(4C)/Cu(4B)···Cu(3C) but not to the polymer stepwise interactions involving Cu(1)···Cu(1A)/Cu(2)···Cu(2B) [Fig. 2(b)]. Once more cross-bipyrazole couplings within **2** are zero. Systematic and careful variation of the three intermolecular 'cross' J values were made and small improvement over eqn. (1) was obtained for $2J_{3B,4C} = -20 \text{ cm}^{-1}$, that is one of the sides of the parallelogram shown in Fig. 2(b) which involves Cu(3B)O(5B)Cu(4C) bridging. Even so, crossing of the observed and calculated χ plots occurs at ca. 250 K. In order to allow for the differences in bridge geometries within each dinuclear half of **2**, we attempted to fit the data to a sum of two independent dimers. The g values were assumed to be the same *viz.* 2.0. The fit was improved in the region 80–230 K compared to a single J model, with best-fit values $2J_1 = -414 \text{ cm}^{-1}$ and $2J_2 = -380 \text{ cm}^{-1}$ (where $2J_1$ and $2J_2$ represent either $2J_{12}$ and $2J_{34}$ or *vice versa*), but again, crossing of calculated and observed curves occurred above 250 K with calculated values being lower than observed values. In view of the experience gained with the fitting of the data for **1**, and the lack of an observed maximum in χ for **2** on which more sensitive testing could be performed, it was decided not to pursue a combination of two independent dimers plus intermolecular coupling of the Hatfield and Inman or other chain types.

In summary, the magnetic behaviour of **2** is generally consistent with medium strength intramolecular antiferromagnetic coupling within the [Cu(1)···Cu(2)] and [Cu(3)···Cu(4)] pairs, and between which there is no cross-mdpz coupling. There is a small difference in size of the $2J$ values in each pair with both being larger than in the analogous dinuclear complex containing the same Schiff-base backbone and a μ -pyrazolate bridge [Cu₂L(pz)] (-240 cm^{-1}).¹⁸ There is some evidence for very weak antiferromagnetic intermolecular coupling but this has not been fully quantified. The magnetic behaviours of com-

plexes **1** and **2** are generally very similar with only some small differences observed in the shape of the χ/T plot above 250 K and with a larger $2J$ value deduced for **1**. We will report separately on similar structure/magnetism investigations of mixed-metal di- and tetra-nuclear derivatives of these ligand frameworks.²¹

Acknowledgements

This research was supported by funds from the Australian Research Council and Trinity College Academic Development Research fund.

References

- (a) S. J. Lippard and J. M. Berg, *Principles of Bioinorganic Chemistry*, University Science Books, Mill Valley, CA, 1994; (b) W. Kaim and B. Schwerderski, *Bioinorganic Chemistry: Inorganic Elements in the Chemistry of Life*, John Wiley, Chichester, 1994; (c) R. H. Holm, P. Kennepohl and E. I. Solomon, *Chem. Rev.*, 1996, **96**, 2239.
- (a) E. I. Solomon, U. M. Sandaram and T. E. Machonkin, *Chem. Rev.*, 1996, **96**, 2563; (b) *Multi-copper Oxidases*, ed. A. Messerschmidt, World Scientific, Singapore, 1997.
- J. B. Howard and J. C. Rees, *Chem. Rev.*, 1996, **96**, 2965.
- (a) A. J. Blake, N. R. Champness, P. Hubberstey, W. S. Li, M. A. Withersby and M. Schroder, *Coord. Chem. Rev.*, 1999, **183**, 177 and references therein; (b) P. N. W. Baxter, J.-M. Lehn, G. Baum and D. Fenske, *Chem. Eur. J.*, 1999, **5**, 102; (c) P. N. W. Baxter, J.-M. Lehn, G. Baum, B. O. Kneisel and D. Fenske, *Chem. Eur. J.*, 1999, **5**, 113.
- (a) D. E. Fenton, *Chem. Soc. Rev.*, 1999, **28**, 159; (b) H. Okawa, H. Furutachi and D. E. Fenton, *Coord. Chem. Rev.*, 1998, **174**, 51.
- (a) J. C. Dutton, G. D. Fallon and K. S. Murray, *J. Chem. Soc., Chem. Commun.*, 1990, 64; (b) G. D. Fallon, A. Markiewicz, K. S. Murray and T. Quach, *J. Chem. Soc., Chem. Commun.*, 1991, 198; (c) K. Bertonecello, G. D. Fallon, K. S. Murray and E. R. T. Tiekink, *Inorg. Chem.*, 1991, **30**, 3562; (d) P. E. Kruger, B. Moubaraki, K. S. Murray and E. R. T. Tiekink, *J. Chem. Soc., Dalton Trans.*, 1994, 2129; (e) P. E. Kruger, B. Moubaraki and K. S. Murray, *Polyhedron*, 1997, **16**, 2659.
- P. E. Kruger, G. D. Fallon, B. Moubaraki and K. S. Murray, *J. Chem. Soc., Chem. Commun.*, 1992, 1726.
- P. E. Kruger, G. D. Fallon, B. Moubaraki, K. J. Berry and K. S. Murray, *Inorg. Chem.*, 1995, **34**, 4808.

- 9 G. M. Sheldrick, SHELXTL PLUS, Revision 3.4, Siemens Analytical X-ray Instrument, Inc., Madison, WI, 1988.
- 10 W. Mazurek, Ph.D. Thesis, La Trobe University, 1982.
- 11 E. Knövenagel, *Chem. Ber.*, 1903, **36**, 2136.
- 12 W. L. Mosby, *J. Chem. Soc.*, 1957, 3997.
- 13 W. Mazurek, K. J. Berry, K. S. Murray, M. J. O'Connor, M. R. Snow and A. G. Wedd, *Inorg. Chem.*, 1982, **21**, 3071.
- 14 A. B. P. Lever, *Inorganic Electronic Spectroscopy*, Elsevier, Amsterdam, 1968, p. 359.
- 15 M. A. Monge, E. G. Puebla, J. Elguero, C. Toiron, W. Meutermans and I. Sobrados, *Spectrochim. Acta, Part A*, 1994, **50**, 727.
- 16 (a) R. J. Butcher, G. Diven, G. Erikson, G. Mockler and E. Sinn, *Inorg. Chim. Acta*, 1986, **123**, L17; 1986, **123**, L55; (b) Y. Nishida and S. Kida, *Inorg. Chem.*, 1988, **27**, 447; (c) T. N. Doman, D. E. Williams, J. F. Banks, R. M. Buchanan, H.-R. Chang, R. J. Webb and D. N. Hendrickson, *Inorg. Chem.*, 1990, **29**, 1058.
- 17 B. Bleaney and K. D. Bowers, *Proc. R. Soc. London, Ser. A*, 1952, **214**, 451.
- 18 W. Mazurek, B. J. Kennedy, K. S. Murray, M. J. O'Connor, J. R. Rodgers, M. R. Snow, A. G. Wedd and P. R. Zwack, *Inorg. Chem.*, 1985, **24**, 3258.
- 19 W. E. Hatfield and G. W. Inman, *Inorg. Chem.*, 1969, **8**, 1366.
- 20 (a) J. Lewis and R. A. Walton, *J. Chem. Soc. A*, 1966, 1559; (b) K. S. Murray, *Adv. Inorg. Chem.*, 1995, **43**, 261.
- 21 S. C. Courtney, G. D. Fallon, P. E. Kruger, B. Moubaraki and K. S. Murray, to be submitted. See also: P. E. Kruger, F. Launay and V. McKee, *Chem. Commun.*, 1999, 639.

Paper a908177a